

---

# JOURNAL OF THE AMERICAN CHEMICAL SOCIETY

---

## Dipole Formation and Solvent Electrostriction in Subtilisin Catalysis

Peter C. Michels,<sup>†,‡</sup> Jonathan S. Dordick,<sup>\*,§</sup> and Douglas S. Clark<sup>\*,†</sup>

Contribution from the Department of Chemical and Biochemical Engineering, University of Iowa, Iowa City, Iowa, 52242, and Department of Chemical Engineering, University of California, Berkeley, California 94720

Received May 1, 1997<sup>⊗</sup>

**Abstract:** The transition state for subtilisin-catalyzed transesterification was probed by high-pressure kinetic studies in solvents spanning a wide range of dielectric constants. The electrostatic model of Kirkwood described the solvent effects and gave a lower limit of  $31 \pm 1.5$  Debye for the dipole moment of the transition state. This value remained constant in a wide range of polar and apolar solvents, indicating that the catalytic triad of subtilisin is remarkably robust. Despite the highly polar transition state, substantial rate enhancements relative to the uncatalyzed reaction were measured in highly apolar solvents such as hexane; this is the first report of such an extreme disparity between transition-state and solvent polarities. Moreover, the solvent dependence of the activation volume implies a low effective dielectric of the polypeptide chain in the active site and substantial penetration of the active site by solvent. Kirkwood's model was also used to quantify the effect of an active-site mutation on the transition-state dipole moment. These results illustrate that the electrostatic model combined with high-pressure kinetics can provide unique information on the basic properties of enzyme reaction processes and can be useful in predicting solvent effects on enzyme reaction rates.

### Introduction

The structure and function of serine proteases in nonaqueous media have recently been examined by a variety of techniques. For example, solid-state NMR,<sup>1,2</sup> ESR,<sup>3</sup> deuterium isotope analysis,<sup>4</sup> and crystallographic studies<sup>5-7</sup> on serine proteases suggest that the structure and catalytic mechanism of these enzymes is retained in a wide variety of organic solvents. In

particular, kinetic isotope effects observed for transesterifications catalyzed by subtilisin Carlsberg indicated that the transition state structure was independent of the organic solvent.<sup>4</sup> Preservation of the transition state was also suggested by solid-state MAS <sup>15</sup>N-NMR spectra of a serine protease from *Lysobacter enzymogenes*, which revealed that the unique tautomeric structure and hydrogen bonding interactions essential for function of the catalytic triad were identical in water, acetone, and octane.<sup>1,2</sup> In addition, the crystal structure of cross-linked subtilisin in acetonitrile was essentially identical to the structure of the enzyme in water.<sup>6,7</sup> Despite these results, molecular details on the reaction mechanisms of proteases and other enzymes in nonaqueous media remain scarce.

\* To whom correspondence should be addressed.

<sup>†</sup> University of California.

<sup>‡</sup> Present address: EnzyMed Inc., Iowa City, Iowa 52242.

<sup>§</sup> University of Iowa.

<sup>⊗</sup> Abstract published in *Advance ACS Abstracts*, September 15, 1997.

(1) Burke, P.; Griffin, R. G.; Klibanov, A. M. *J. Am. Chem. Soc.* **1989**, *111*, 8290.

(2) Burke, P. A.; Griffin, R. G.; Klibanov, A. M. *J. Biol. Chem.* **1992**, *267*, 20057.

(3) Affleck, R.; Xu, Z.-F.; Suzawa, V.; Focht, K.; Clark, D. S.; Dordick, J. S. *Proc. Natl. Acad. Sci. U.S.A.* **1992**, *89*, 1100.

(4) Adams, K. A. H.; Chung, S., et al. *J. Am. Chem. Soc.* **1990**, *112*, 9418.

(5) Yennawar, N. J.; Yennawar, H. P.; Farber, G. K. *Biochemistry* **1994**, *33*, 7326.

(6) Fitzpatrick, P. A.; Steinmetz, A. C. U.; Ringe, D.; Klibanov, A. M. *Proc. Natl. Acad. Sci. U.S.A.* **1993**, *90*, 8653.

(7) Fitzpatrick, P. A.; Ringe, D.; Klibanov, A. M. *Biochem. Biophys. Res. Comm.* **1994**, *198*, 675.

High-pressure kinetic studies, although not widely utilized, can be very valuable for investigating the mechanisms of enzymatic reactions in aqueous solution, especially when other methods of mechanistic analysis prove insufficient.<sup>8–10</sup> The key parameter governing the effect of pressure on the rate of a chemical reaction is the activation volume,  $\Delta V^\ddagger$ . In general, bond formation, charge development, and steric hindrance during the rate-controlling step make negative contributions to the activation volume,<sup>11,12</sup> whereas the reverse processes have the opposite effect. In reactions that proceed through a charged or partially charged transition state, the resulting electric field induces electrostriction of the solvent, causing a reduction in volume. Solvent effects have thus been used to infer transition-state properties of many organic reactions.<sup>11–17</sup> With one exception, however, solvent effects on activation volumes of enzyme reactions have not been explored.<sup>18</sup>

### Underlying Theory

The interpretation of charge formation in reaction pathways has been greatly aided by the fundamental analyses of Born<sup>19</sup> and Kirkwood.<sup>20</sup> In particular, Kirkwood generalized Born's original treatment of charge solvation to systems containing arbitrary distributions of charge centers. From this work, the electrostatic Gibbs energy upon transfer of a mole of dipoles of moment  $\mu$  from a vacuum (i.e.,  $\epsilon = 1$ ) into a spherical cavity of radius  $r$ , inside an isotropic continuum of dielectric constant  $\epsilon$ , can be evaluated (eq 1):

$$\Delta G_E = -N_A \left( \frac{\mu^2}{r^3} \right) \left[ \frac{(\epsilon - 1)}{(2\epsilon + 1)} \right] \quad (1)$$

The quantity in brackets is the dielectric constant factor  $q$ . Equation 1 can also be used to evaluate the electrostatic Gibbs energy of activation for a chemical reaction,<sup>21</sup> e.g., the reaction  $S \rightarrow P$  that proceeds through the transition state  $S^\ddagger$ . Furthermore, the pressure derivative of eq (1) describes the electrostriction caused by the net dipole moment of the transition state and represents the electrostatic contribution to the activation volume of the reaction.<sup>14</sup> The total activation volume,  $\Delta V^\ddagger$ , can thus be expressed as a combination of nonelectrostrictive and electrostrictive terms (eq 2), as presented in ref 14:

$$\Delta V^\ddagger = \Delta V_0^\ddagger - N_A \left[ \frac{\mu_{S^\ddagger}^2}{r_{S^\ddagger}^3} - \frac{\mu_S^2}{r_S^3} \right] \left( \frac{\partial q}{\partial p} \right) \quad (2)$$

In eq (2)  $\Delta V_0^\ddagger$  represents the activation volume in the absence of electrostriction, and the term in brackets contains the dipole moment of the transition state  $\mu_{S^\ddagger}$ . Kirkwood's electrostatic model has been useful in high-pressure mechanistic studies of

Metshutkin reactions,<sup>15</sup> Diels–Alder reactions,<sup>16,22</sup>  $S_N1$  substitutions,<sup>17</sup> and many other classes of organic reactions.<sup>13,14</sup> Because of the limiting assumptions inherent in the derivation (most notably the exclusion of nonelectrostatic interactions, e.g., van der Waals forces and hydrogen bonding), deviations from the theory for some solvents are not unusual.<sup>15,16</sup> However, recent molecular dynamics simulations<sup>23</sup> have revealed that the Born–Kirkwood dielectric continuum representation of the reaction solvent agrees much more closely with microscopic models than previously thought, although its application to enzyme reactions has not been considered previously. This is the focus of the current study.

### Kirkwood Analysis of Enzymatic Reactions

The activation volume for an enzymatic reaction can be related to its catalytic efficiency,  $k_{cat}/K_m$ , through an expression analogous to eq 2

$$-RT \left( \frac{\partial \ln \left( \frac{k_{cat}}{K_m} \right)}{\partial P} \right)_T = \Delta V^\ddagger = \Delta V_0^\ddagger - N_A \Delta \left( \frac{\mu^2}{r^3} \right) \left( \frac{\partial q}{\partial p} \right) \quad (3)$$

where

$$\Delta \left( \frac{\mu^2}{r^3} \right) = \left( \frac{\mu_{ES^\ddagger}^2}{r_{ES^\ddagger}^3} - \frac{\mu_S^2}{r_S^3} - \frac{\mu_E^2}{r_E^3} \right) \quad (4)$$

and  $ES^\ddagger$ ,  $S$ , and  $E$  denote the enzymic transition state, substrate, and enzyme, respectively. From eq 3, plotting the experimental  $\Delta V^\ddagger$  versus  $(\partial q/\partial P)$  for various solvents should yield a straight line, with a slope of  $-N_A \Delta(\mu^2/r^3)$  and a y-intercept of  $\Delta V_0^\ddagger$ . This intercept consists of the intrinsic structural contributions to  $\Delta V_0^\ddagger$ , such as changes in bonding and bond lengths during formation of the transition state as well as nonelectrostrictive solvent contributions that are common among all the solvents used. Neglected from this description are pressure effects arising from any specific contributions from a given solvent, such as hydrogen bonding, solvent participation in the transition state, or solvophobic effects. These omissions are difficult to evaluate independently and often result in deviations from the Kirkwood plot, underscoring the approximate nature of this analysis. Nevertheless, a strong solvent dependence of the activation volume signals a highly polar transition state and, in the absence of strong specific solvent effects, provides the basis for estimating the transition-state dipole moment.

### Materials and Methods

Catalytic efficiencies were determined for subtilisin-catalyzed transesterification in various organic solvents. Twice-crystallized and lyophilized subtilisin Carlsberg (Sigma Chemical, St. Louis, MO), and subtilisin BPN' (wild-type and the active-site mutant, G166N, generously provided by Dr. Thomas Graycar at Genencor International, S. San Francisco, CA) were activated for catalysis in organic solvents by freeze-drying from a 10 mg/mL aqueous solution (10 mM phosphate buffer, pH 7.8) for 42 h at 40 mTorr. All organic solvents were of the highest grade commercially available and were dehydrated by storing over 3 Å molecular sieves (Linde) for at least 24 h immediately prior to use. Water concentrations of the solvent were measured prior to each set of reactions by Karl Fischer titration.

In a typical reaction, 925  $\mu\text{L}$  of a 0.27 mg/mL suspension of subtilisin in the reaction solvent was added to a stainless steel type 316 pressure bomb (internal volume, 1.5 mL) and preheated to 30.0 °C in a forced

(8) Rodgers, K. K.; Pochapsky, T. C.; Sligar, S. G. *Science* **1988**, *240*, 1657.

(9) Rasper, J.; Kauzmann, W. *J. Am. Chem. Soc.* **1962**, *84*, 6835.

(10) Chrystomallis, G. S.; Torgerson, P. M.; Drickamer, H. G.; Weber, G. *Biochemistry* **1982**, *20*, 3955.

(11) van Eldik, R.; Asano, T.; le Noble, W. J. *Chem. Rev.* **1989**, *89*, 549.

(12) Weale, K. E. *Chemical Reactions at High Pressures*; Spon: London, 1967; pp 1–349.

(13) Brower, K. R.; Chen, J. S. *J. Am. Chem. Soc.* **1965**, *87*, 3396.

(14) Eckert, C. A. *Ann. Rev. Phys. Chem.* **1972**, *23*, 239.

(15) Hartmann, H.; Brauer, H. D.; Kelm, H.; Rinck, G. Z. *Physik Chem.* **1968**, *61*, 53.

(16) Greiger, R. A.; Eckert, C. A. *Trans. Faraday Soc.* **1970**, *66*, 2579.

(17) Kotowsky, R.; Palmer, D. A.; Kelm, H. *Inorg. Chem.* **1970**, *18*, 2555.

(18) Kim, J.; Dordick, J. S. *Biotechnol. Bioeng.* **1993**, *42*, 772.

(19) Born, M. *Z. Phys.* **1920**, *1*, 45.

(20) Kirkwood, J. G. *J. Chem. Phys.* **1934**, *2*, 351.

(21) Stearn, A. E.; Eyring, H. *Chem. Rev.* **1941**, *29*, 509.

(22) McCabe, J. R.; Eckert, C. A. *Ind. Eng. Chem. Fundam.* **1974**, *13*, 168.

(23) Roux, B.; Yu, H.-A.; Karplus, M. *J. Phys. Chem.* **1990**, *94*, 4683.

air oven (Blue M Corp, Blue Island, IL). The suspension was maintained by sonication during sampling of the stock enzyme solution. The transesterification reaction of acetyl-L-phenylalanine ethyl ester (APEE) was then initiated by adding 75  $\mu\text{L}$  of a freshly prepared stock solution of APEE in *n*-propanol. The final concentrations of the substrates were 1 M *n*-propanol and 5–40 mM APEE in a 1 mL total liquid volume. Pressurization was achieved with oxygen-free helium and was complete within 20–30 s of the substrate being added to the pressure bomb. In a control experiment to investigate potential heating upon pressurization, pressurization of the water-filled bomb to 500 atm over 5 s caused a temperature rise of less than 1  $^{\circ}\text{C}$ , measured with a high-pressure thermocouple.

Samples were periodically withdrawn from the reactor, and the formation of acetyl-L-phenylalanine propyl ester was followed by GC-MS using a 25 m, 95% methyl–5% biphenyl capillary column (Hewlett-Packard). There was no measurable reaction in hexane in the absence of enzyme and hence no detectable product. Therefore, a lower limit of the enzymatic rate enhancement relative to the uncatalyzed reaction at room temperature was determined by dividing  $k_{\text{cat}}/K_{\text{m}}$  ( $4.6 \text{ M}^{-1} \text{ s}^{-1}$ ) by the rate constant for the uncatalyzed reaction estimated from the measured detection limit of the gas chromatograph for acetyl-L-phenylalanine propyl ester ( $2.2 \times 10^{-10} \text{ M}^{-1} \text{ s}^{-1}$ ). The estimated lower limit of the rate enhancement was thus ca.  $2.1 \times 10^{10}$ .<sup>24</sup>

The initial rates increased linearly with substrate concentration, indicating that the reaction followed first-order kinetics over the substrate range tested (5–40 mM). To convert the reaction velocities into the kinetic parameter  $k_{\text{cat}}/K_{\text{m}}$ , the fraction of active sites available in the suspended subtilisin powders (which were prepared exactly the same way for all experiments) was assumed to be 15%, independent of pressure. This value is based upon our previous active-site titration measurements for this enzyme in a variety of solvents and is in agreement with the results of Affleck et al.<sup>3</sup> for the same lyophilization procedure. The relatively low fraction of competent active sites is reportedly due to the irreversible (in organic solvents) partial unfolding of the native enzyme structure during the lyophilization process.<sup>25,26</sup> Once the sonicated powders are suspended in organic solvent, no treatment, including pressurization, has been shown to induce irreversibly denatured enzyme to refold to the native and active form. Hence the assumption that the competent active-site concentration is independent of pressure.

Because the  $k_{\text{cat}}/K_{\text{m}}$  values are reported in pressure-dependent units of  $\text{M}^{-1}\cdot\text{s}^{-1}$ , compression of solvent must be accounted for by correcting the calculated activation volumes by  $RT\beta_{\text{T}}$ , where  $\beta_{\text{T}}$  is the isothermal compressibility of the solvent.<sup>27</sup> For subtilisin-catalyzed transesterification in organic solvents, this adjustment typically resulted in a correction of 3–4  $\text{cm}^3/\text{mol}$ .

## Results and Discussion

Figure 1 plots the catalytic efficiencies in hexane versus pressure. As is often the case, this plot exhibits slight curvature, which is typically described by a quadratic series in pressure.<sup>12</sup> The value for  $\Delta V^{\ddagger}$  in hexane was obtained from Figure 1 by evaluating the slope of this quadratic at 1 bar.<sup>12,13</sup> The uncatalyzed reaction was very slow at room temperature (no measurable product in hexane after 48 h). However, cursory rate measurements of the uncatalyzed reaction in hexane at 150  $^{\circ}\text{C}$  provided an upper limit for the reaction rate of  $\sim 0.4 \mu\text{M}/\text{h}$  and showed very little effect of pressure ( $\Delta V^{\ddagger} \sim -5 \text{ mL}/\text{mol}$  at 100  $^{\circ}\text{C}$  based on a comparison of the uncatalyzed reaction rates at 1 and 500 bar).

Effective activation volumes for the transesterification of

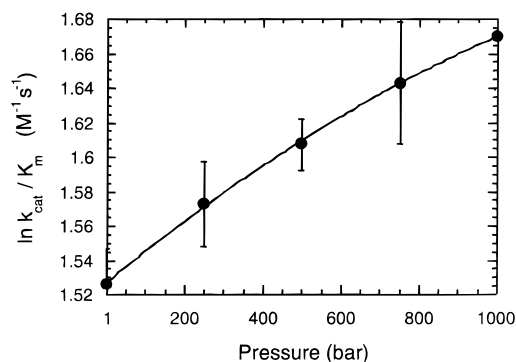


**Figure 1.** Catalytic efficiency of subtilisin Carlsberg measured for transesterification in hexane as a function of pressure. The curve represents a quadratic fit to the data. The activation volume was calculated from the slope of the quadratic at 1 bar.

APEE are plotted against  $(\partial q/\partial P)$  in Figure 2.<sup>28</sup> Values of  $(\partial q/\partial P)$  were calculated from literature data for the dependence of the solvent dielectric constant on pressure.<sup>29–32</sup> As shown by the plot, pressurization of subtilisin Carlsberg significantly increased or decreased catalytic efficiencies for transesterification, depending on the solvent. For example,  $k_{\text{cat}}/K_{\text{m}}$  in propyl ether increased from  $0.44 \text{ M}^{-1}\cdot\text{s}^{-1}$  at ambient pressure to  $4.6 \text{ M}^{-1}\cdot\text{s}^{-1}$  at 1000 bar (i.e.,  $\Delta V^{\ddagger} = -55 \text{ mL}/\text{mol}$ ), a factor of greater than 10. In contrast, the apparent activation volume in acetone is 58  $\text{mL}/\text{mol}$ , which corresponds to a 10-fold reduction in  $k_{\text{cat}}/K_{\text{m}}$  at 1000 bar.

The good linear correlation between  $\Delta V^{\ddagger}$  and  $(\partial q/\partial P)$  for the various solvents demonstrates the strong participation of electrostatic effects during the formation of the transition state. From eq 3, the slope of the line equals  $-N_{\text{A}}\Delta(\mu^2/r^3)$ . Estimating the value of  $r$  from the known geometry of the transition state thus enables one to calculate the apparent change of polarity for the formation of the transition-state acyl–enzyme complex (eq 4). The most likely source of this polarity change, based on the widely accepted charge-transfer mechanism of serine proteases in water, is the developing charge on both His<sub>64</sub> and the substrate carboxyl group during formation of the transition state.

In eq (4), the term  $\mu_{\text{s}}^2/r_{\text{s}}^3$  can be calculated for the substrate in its ground state using standard computational methods.<sup>33</sup> For APEE in organic solvents, a radius of 3.9  $\text{\AA}$  was calculated from a van der Waals volume of 184  $\text{\AA}^3$ .<sup>34</sup> Optimizing the structure of APEE by molecular simulation in a low dielectric and calculating its dipole moment using the method of Pullman

(28) We did not compare ester hydrolysis in aqueous solution to transesterification in organic solvents for two primary reasons. First, the two types of reactions have different rate-limiting steps. The rate-controlling step for subtilisin-catalyzed ester hydrolysis is deacylation (Bonneau, P. R.; Graycar, T. P.; Estell, D. A.; Jones, B. J. *J. Am. Chem. Soc.* **1991**, *113*, 1026), whereas the rate-controlling step for transesterification in organic solvents is acylation (Wangikar, P. P.; Graycar, T. P.; Estell, D. A.; Clark, D. S.; Dordick, J. S. *J. Am. Chem. Soc.* **1993**, *115*, 12231. Chatterjee, S.; Russell, A. J. *Biotechnol. Bioeng.* **1992**, *40*, 1069.) Moreover, water differs in its mechanism of electrostatic solvation compared with more apolar solvents (Whalley, E. *J. Chem Phys.*, **1963**, *38*, 1400.) and commonly engages in nonelectrostrictive interactions. These effects often cause deviations from the Kirkwood model for electrostriction (Isaacs, N. *Liquid Phase High Pressure Chemistry*; John Wiley & Sons: Chichester, 1981 pp 181–343. Hamann, S. D. *Mod. Asp. Electrochem.* **1972**, *9*, 47.)

(29) Brazier, D. W.; Freeman, G. R. *Canadian J. Chem.* **1969**, *47*, 893.

(30) Owen, B. B.; Stuart R. Brinkley, *J. Phys. Rev.* **1943**, *64*, 32.

(31) Schornack, L. G.; Eckert, C. A. *J. Phys. Chem.* **1970**, *74*, 3014.

(32) Skinner, J. F.; Cussler, E. L.; Fuoss, R. M. *J. Phys. Chem.* **1968**, *72*, 1057.

(33) Clark, M.; Cramer, R. D.; van Opdenbosch, N. *J. Comput. Chem.* **1989**, *10*, 982.

(34) Cox, P. J. *J. Chem. Educ.* **1982**, *59*, 275.

(24) This estimate, while only approximate, is comparable to the value reported previously for a similar transesterification reaction catalyzed by subtilisin in octane (Zaks, A.; Klivanov, A. M. *J. Biol. Chem.* **1988**, *263*, 3194).

(25) Desai, U. R.; Osterhout, J. J.; Klivanov, A. M. *J. Am. Chem. Soc.* **1994**, *116*, 9420.

(26) Desai, U. R.; Klivanov, A. M. *J. Am. Chem. Soc.* **1995**, *117*, 3940.

(27) le Noble, W. J. *Rev. Phys. Chem. Jpn.* **1980**, *50*, 207.

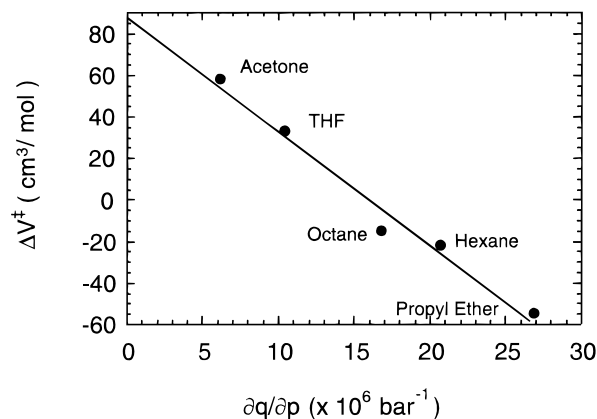


**Figure 2.** Kirkwood plot for the apparent activation volumes of subtilisin-catalyzed transesterification in organic solvents.

and Berthod<sup>35</sup> gave  $\mu_s = 5.99$  Debye. Based on these values,  $\mu_s^2/r_s^3 = 6.05 \times 10^{-13}$  ergs. Furthermore, the dipole of the catalytic triad in the ground state of subtilisin is expected to be negligible in comparison to the dipole of the charged transition state; hence, the ground-state dipole of the active site has been neglected. Neglecting this term in the right-hand side of eq (4) leads to a lower limit for the value of  $\mu_{ES}^\ddagger$ .

The separation of charge in the transition state can be approximated as the distance between the  $N^{\delta 1}$  atom of His<sub>64</sub> and the average position of hydrogen bonds from Asn<sub>155</sub> that delocalize the charge of the oxyanion group of the transition state. Based on the X-ray crystal structure of subtilisin Carlsberg inhibited by the transition-state analog *N*-*tert*-butoxycarbonyl-*l*-pro-phe-*O*-benzoylhydroxylamine,<sup>36</sup> this charge separation is  $9.3 \pm 0.3 \text{ \AA}$  (Figure 3). The error range of  $\pm 0.3 \text{ \AA}$  represents the accuracy to which atoms can be located, given the  $1.8 \text{ \AA}$  resolution of the crystal structure.<sup>36</sup> Although this crystal structure was obtained for the enzyme in aqueous solution, the crystal structures of cross-linked subtilisin Carlsberg in nearly anhydrous acetonitrile and in water are essentially identical to within the limits of their resolution.<sup>6,7</sup> Likewise, the crystal structure of the serine protease chymotrypsin in hexane exhibits only minor perturbations from the crystal structure in aqueous solution.<sup>5</sup> Thus, an aqueous structure can be assumed to describe the structure of subtilisin in hexane. Therefore, in terms of the Kirkwood model, the separation of charge in the transition state can be viewed as a dipole consisting of positive and negative charges of 0.7 charge units each separated by a distance of  $9.3 \text{ \AA}$  (1 charge unit =  $4.8029 \times 10^{-10}$  esu).

A charge separation of  $9.3 \pm 0.3 \text{ \AA}$  leads to a value of  $31 \pm 1.5$  Debye for  $\mu_{ES}^\ddagger$ , which represents a lower limit for the dipole moment of the transition-state acyl-enzyme complex. Note that eq 3 predicts that for a line of constant slope, the dipole moment varies with  $r$  raised to the  $3/2$  power. Thus, varying the charge separation from 8 to  $10 \text{ \AA}$  (i.e.,  $r$  from 4 to  $5 \text{ \AA}$ ) leads to a range of dipole moments from 25 to 35 Debye. However, the linearity of Figure 2 illustrates that the transition state dipole moment is independent of the solvent. Moreover, the charge separation of  $9.3 \text{ \AA}$  is based on current knowledge of the enzyme's transition state structure and recent crystallographic data for the protein in aqueous and organic solvents.

This value of  $\mu_{ES}^\ddagger$  determined from the Kirkwood plot is comparable to the value of 35 Debye calculated for subtilisin in aqueous solution by Lamotte-Brasseur et al.<sup>37</sup> using computer

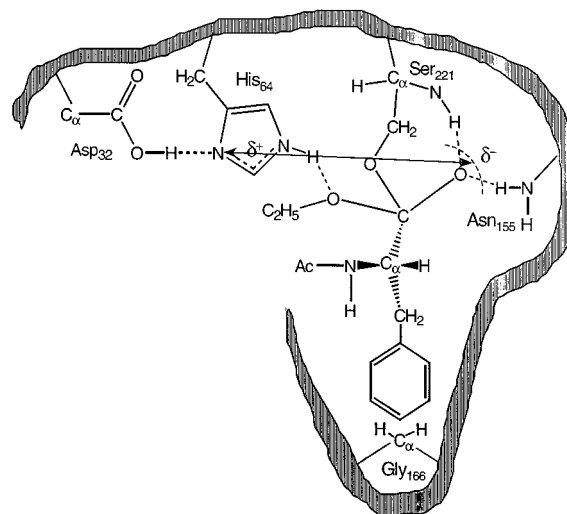


**Figure 3.** Hypothetical transition state for transesterification of APEE catalyzed by subtilisin Carlsberg, with the  $9.3 \text{ \AA}$  charge separation of the effective dipole indicated by the arrow. The dashed arc represents the average position of hydrogen bonds from Asn<sub>155</sub> that delocalize the charge of the oxyanion group of the transition state. For further details, see text.

simulation of electrostatic potential integrals on the quantum level. These calculations showed that generation of the electrostatic field centered around the protonated active-site His<sub>64</sub> and the electrophilic "oxyanion hole" created between the backbone NH of the catalytic Ser<sub>221</sub> and the side-chain amide group of Asn<sub>155</sub>. The formation of charge was promoted by the interaction of at least 10 additional residues in a  $7 \text{ \AA}$  sphere around the active site. This illustrates the dramatic cooperativity of residues in proximity to the catalytic serine, leading to the high catalytic efficiency of the enzyme macromolecule. Interestingly, the inclusion of 25 solvent (water) molecules in the active site had little effect on charge development in the transition state, suggesting that water plays no direct role in the formation of the transition state. That the inclusion of water molecules in the calculations of Lamotte-Brasseur et al.<sup>37</sup> had little effect on the maximum amplitude of the local electrostatic potential supports our contention that water need not be present for significant charge to be generated in the active site of subtilisin during catalysis.

If electrostatic damping was the only role played by the solvent in subtilisin catalysis, the integrated form of eq (3) predicts that a plot of  $\ln(k_{cat}/K_m)$  versus  $q$  for various solvents should yield a straight line of slope  $(N_A/RT)\Delta(\mu^2/r^3)$ . As illustrated in Figure 4, this is not the case.<sup>38</sup> The dashed line in Figure 4 represents the theoretical effect of simple electrostatic solvation on the reaction rate, assuming a transition-state dipole of 31 Debye. The line was forced through the value of  $k_{cat}/K_m$  determined for the hydrolysis of APEE in subtilisin's native solvent, water. The apparently random scatter of data for the organic solvents suggests that a nonelectrostrictive solvent effect(s) influences catalysis in these solvents. In addition, the linear correlation of activation volumes with  $(\partial q/\partial P)$  in Figure 2 indicates that these additional solvent effects are independent of pressure. These observations highlight the inherent limitations of the Kirkwood model and provide strong evidence that nonelectrostrictive effects can have a profound influence on catalytic function. In this case, there are nonelectrostrictive contributions to the activation free energy, which do not affect the activation volume.

(35) Berthod, H.; Pullman, A. *J. Chem. Phys.* **1965**, *62*, 942.

(36) Steinmetz, A. C. U.; Demuth, H.-U.; Ringe, D. *Biochemistry* **1994**, *33*, 10535.

(37) Lamotte-Brasseur, J.; Dive, G.; Dehareng, D.; Ghuyen, J. M. *J. Theor. Biol.* **1990**, *145*, 183.

(38) Essential data on the effect of pressure on the dielectric constant ( $\partial\epsilon/\partial P$ ) were available for a limited number of solvents; hence, more solvents were included for the modeling in Figure 4 than in Figure 2.

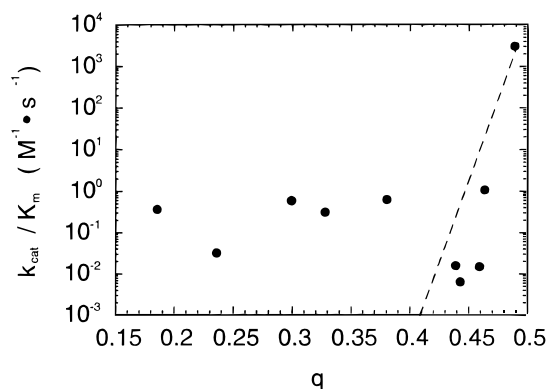


**Figure 4.** Catalytic efficiencies of subtilisin BPN' versus the dielectric constant factor,  $q$ , of the solvent. Note that the values (excluding the value for water) span at least two orders of magnitude. The dashed line represents the theoretical prediction based on the integrated form of eq 3, assuming a transition-state dipole of 31 Debye. The deviation of the data from the prediction is evidence that nonelectrostrictive effects have a strong influence on subtilisin catalysis in most if not all of these solvents. Solvents ( $q$ ,  $k_{\text{cat}}/K_m$  in  $\text{M}^{-1}\cdot\text{s}^{-1}$ ) are as follows: hexane (0.186, 0.43); toluene (0.236, 0.030); propyl ether (0.300, 0.44); isopropyl ether (0.329, 0.26); *tert*-amyl alcohol (0.381, 0.60); 2-heptanone (0.439, 0.018); 3-heptanone (0.444, 0.0064); cyclohexanone (0.459, 0.016); acetone (0.464, 0.95); and water (0.49, 2800).

If nonelectrostrictive effects of the solvent on the enzyme could be implicitly accounted for, the agreement of the activation free-energy data with the Kirkwood model should improve. This postulate can be examined by replotting the data of Xu et al.<sup>39</sup> for the transesterification activity of the active-site mutant of subtilisin BPN', G166N. ( $\text{Gly}_{166}$  is located at the far end of the open cleft of the  $S_1$  acyl binding pocket of the enzyme<sup>40</sup>). Because the data for the active-site mutant in various solvents can be normalized by the catalytic efficiency of the wild type, solvent effects distinct from the active site can be factored out. Such a plot (Figure 5) exhibits good agreement with the predicted linear dependence of  $\ln(k_{\text{cat}}/K_m)$  versus  $q$ . That the mutant differs from the wild type only in the active site implies that the solvent effects on the activation volume (Figure 2) and reaction rate (Figure 5) do indeed arise from active-site polarization during catalysis for the enzyme-catalyzed reaction. Furthermore, the agreement of the normalized data with theory indicates that nonelectrostrictive effects act almost exclusively at regions distinct from the enzyme's active site.

The extent to which nonelectrostrictive effects influence subtilisin catalysis warrants further consideration in view of Figures 4 and 5. The Kirkwood model clearly fails to describe the data plotted in Figure 4, where  $k_{\text{cat}}/K_m$  values vary over several orders of magnitude and exhibit no discernible dependence on  $q$ . Thus, whereas the electrostriction model explains reasonably well the pressure dependence of catalysis, it is too simplistic to predict the free energy change during catalysis. However, if nonelectrostrictive effects removed from the active site are accounted for, as they are in the normalized data plotted in Figure 5, the accuracy of the model improves substantially. This indicates that the Kirkwood model offers a reasonable

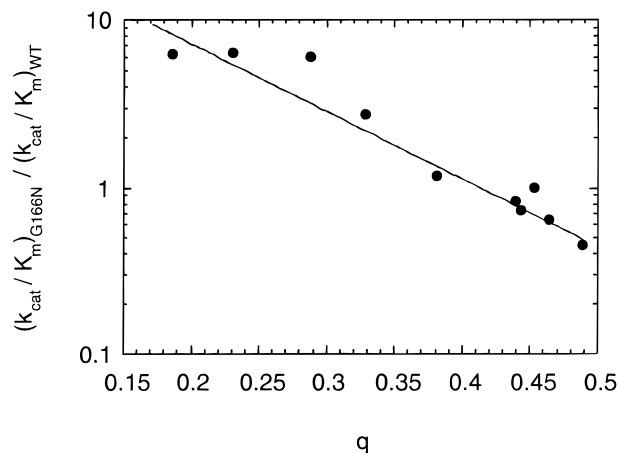


**Figure 5.** Catalytic efficiency of the active-site mutant G166N, normalized by that of wild-type subtilisin BPN', as a function of the dielectric constant factor. The solid line represents the theoretical prediction of the integrated form of eq 3, assuming that the transition-state dipole of G166N is 5.0 Debye less than that of the wild-type.

description of electrostriction effects in the transition state of subtilisin.

From the slope of the plot in Figure 5, the effect of the active-site mutation on transition-state dipole formation can be estimated. The slope of Figure 5 indicates that mutation of  $\text{Gly}_{166}$  to the more polar  $\text{Asn}_{166}$  results in a decrease of roughly 5 Debye in the transition-state dipole strength. This change is consistent with improved catalytic efficiency of the polar mutant relative to the wild-type subtilisin BPN' in low dielectric solvents due to a reduction in the electrostatic energy of dipole formation.

The results reported here support a transition-state model in which the concerted action of several amino acid residues specifically oriented in the active site of subtilisin enables the formation of a strong net dipole during catalysis in organic media. The marked dependence of the activation volume on the solvent suggests solvent penetration of the active site *in the vicinity* of the transition state. The magnitude of the transition-state dipole moment is independent of the bulk solvent, however, indicating that the separation and charge in the transition state remain constant, and solvent does not penetrate the dipole sphere defined by a diameter of 9.3 Å (Figure 3).

In the absence of an enzyme catalyst, reactions that occur through an activated intermediate with a dipole moment greater than 3–6 Debye are very uncommon in apolar solvents. For instance, the rate of the Diels–Alder cycloaddition reaction, which has a transition state dipole moment of between 3–7 Debye, is  $\sim 100$  times slower in isopropyl ether ( $\epsilon = 3.8$ ) than in acetone ( $\epsilon = 20.6$ ).<sup>31</sup> Metschutkin reactions are a dramatic example of a charge-generating organic reaction proceeding through a highly polar ( $\sim 11$  Debye) transition state, but the rate in solvents of dielectric below that of toluene ( $\epsilon = 2.4$ ) is almost negligible, even at high pressures<sup>32</sup> (which accelerate the reaction). Considering the  $\mu^2$  dependence of the electrostatic solvation energy, that enzyme catalysis can proceed through a highly polar transition state ( $\sim 31$  Debye) in extremely apolar solvents such as hexane, with catalytic enhancements relative to the uncatalyzed reaction on the order of  $10^{10}$ , is indeed remarkable and highlights the robustness of the enzyme in maintaining the cooperativity among active-site groups necessary to effect catalysis.

**Acknowledgment.** We thank Joseph O. Rich for assistance in preparing the manuscript. This work was supported by the Army Research Office (DAAH04-94-G-0307).

(39) Xu, Z.-F.; Affleck, R.; Wangikar, P.; Suzawa, V.; Dordick, J. S.; Clark, D. S. *Biotechnol. Bioeng.* **1994**, *43*, 515.

(40) Based on the x-ray crystal structure of subtilisin BPN', the distance between the  $\text{O}^\gamma$  atom of serine 221 and the  $\text{C}^\alpha$  atom at position 166 is 10.6 Å (41). The distance from the  $\text{C}^\alpha$  atom to the  $\text{N}^{\delta 2}$  atom of asparagine is ca. 3.5 Å.

(41) Bott, R.; Ultsch, M.; Kosiakoff, A.; Graycar, T. Katz, B.; Power, S. *J. Biol. Chem.* **1988**, *263*, 7895.